Combinatorial Synthesis of Peptidomimetics Using Digital Microfluidics

Mais J. Jebrail, Naila Assem, Jared M. Mudrik, Michael D.M. Dryden, Kaixiang Lin, Andrei K. Yudin* and Aaron R. Wheeler*

Department of Chemistry, University of Toronto, Toronto ON M5S-3H6, Canada

A microfluidic technique for combinatorial chemical synthesis of peptidomimetics has been developed. The new method is fast, automated and includes an integrated magnetic separation of inorganic catalysts from reaction products. This proof-of-concept study should lead to methods for generating libraries of compounds suitable for screening for bioactivity.

Keywords: digital microfluidics, combinatorial synthesis, peptidomimetics, therapeutics discovery

1. Introduction

Peptidomimetics, or synthetic chain-like molecules designed to mimic peptides, are emerging as important tools in drug discovery [1]. For example, some peptidomimetics act as inhibitors of protease activity and have better pharmacological profiles than their natural peptide counterparts [2]. We recently developed a ligation method to form peptidomimetics that install links between peptide fragments through a peptide bond isostere [3]. This synthetic route was made possible using thioacid peptides and NH aziridine-terminated amino acids, and it addresses some of the key challenges of peptidomimetic ligation, including improved yield, selectivity, and diversity. To find broader utility, it would be helpful to implement this method combinatorially to be able to generate a library of related compounds suitable for screening.

The promise of combinatorial chemical synthesis has been a driving force in the development of microfluidic technology [4]. Microfluidic reactions consume minute amounts of reagents and solvents, and can be carried out at faster rates relative to their macroscale counterparts because of short diffusion distances and rapid heat exchange [5]. The most common format for microfluidic synthesis relies on microfabricated networks of enclosed channels. Such systems have been used for a wide range of applications, including conventional organic synthesis [4, 6], biomaterials [5b, 5c, 7], and nanoparticles [5a, 5d, 8]. The advantages of microchannels are myriad; key among them is being suitable for continuous flow chemistry processes (with inherent benefits for sequential reactions, rapid mixing, access to short-lived intermediates etc. [9]). However, there are also some disadvantages for microchannel synthesis techniques. For example, many microchannel platforms are formed from poly(dimethyl siloxane), a material that is susceptible to degradation in common organic solvents [10]. In addition, control of multiple reagents simultaneously (a feature required for multiplexing) requires pumps, tubing, valves, and/or three-dimensional channel networks that can be difficult to fabricate and operate [4a, 11]. A third disadvantage is the challenge inherent in the removal of solvents and re-dissolution of solids (common steps in synthetic applications). Solid reagents and products can clog microchannels, making reactions difficult to control.

In response to these challenges, we chose an alternative format for automated combinatorial synthesis of peptidomimetics, called digital microfluidics [12]. In digital microfluidics, discrete nL–μL droplets of samples and reagents are controlled in parallel (i.e., moved, merged, mixed, and dispensed from reservoirs) by applying a series of electrical potentials to an array of electrodes coated with a hydrophobic insulator. Recently, digital microfluidics has become popular for applications in chemical synthesis [13]. While such methods are best described as microbatch chemistry rather than flow chemistry, the digital microfluidic format shares many of the advantages of microchannels, with added benefits of inert device materials, control over reagents without pumps, valves, or tubing, and facile handling of both solids and liquids (i.e., there are no channels to clog). However, the technique is still new, and until now, there have been no reports of using digital microfluidics for combinatorial synthesis. Here, we report a digital microfluidic method for combinatorial chemical synthesis of peptidomimetics and related products. In addition, we report the use of an integrated magnetic separation of inorganic catalysts from reaction products.

2. Results and Discussion

The starting reagents used in this work, shown in Figure 1, are two thioacid peptides ($\boldsymbol{A}_{1,2}$) and two NH aziridine-terminated amino acids ($\boldsymbol{B}_{1,2}$). The latter was prepared using the now commercially available amphoteric aziridine aldehydes [14]. We used our new synthetic route [3] to react $\boldsymbol{A}_{1,2}$ and $\boldsymbol{B}_{1,2}$ to form four peptidomimetic products ($\boldsymbol{A}_i$–$\boldsymbol{B}_j$) as shown in Table 1. The digital microfluidic device used for this work, shown in Figure 2a, features ten reagent reservoirs and eighty-eight actuation electrodes dedicated to dispensing, merging, and mixing droplets of reagents and products. Each device handles six different reagents, including the four starting materials, a Raney Nickel catalyst (RaNi), and methanol (MeOH).

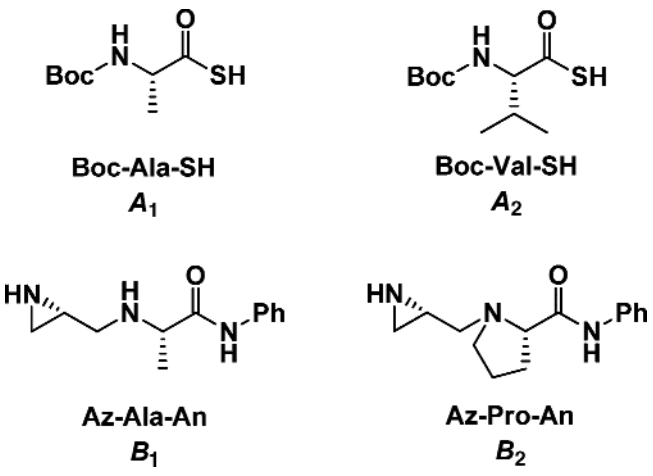

Figure 1. Starting materials used for combinatorial peptidomimetic synthesis: thioacid peptides ($\boldsymbol{A}_{1,2}$) and NH aziridine-terminated amino acids ($\boldsymbol{B}_{1,2}$)

* Author for correspondence: ayudin@chem.utoronto.ca and aaron.wheeler@utoronto.ca

DOI: 10.1556/JFC-D-12-00012

Table 1. Reaction scheme (top) and products (bottom) for the combinatorial synthesis of peptidomimetics

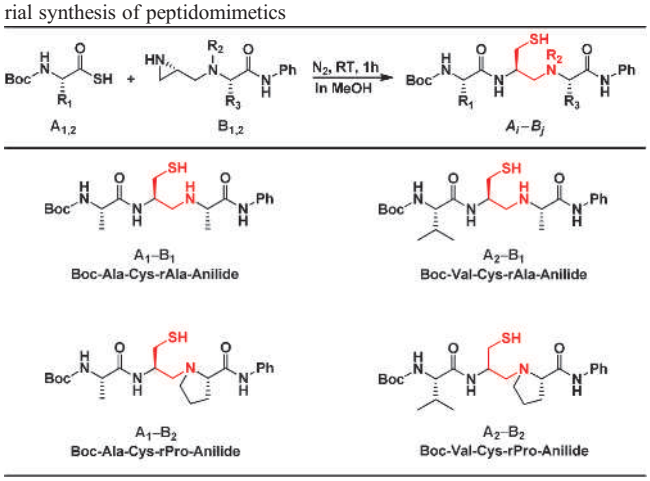

A 16-step digital microfluidic method was developed to facilitate combinatorial synthesis of peptidomimetic products (Figure 2b and c). Figure 3 shows representative mass spectra of A_1–B_1, A_1–B_2, A_2–B_1, and A_2–B_2, with peaks at *m*/*z* 425, *m*/*z* 451, *m*/*z* 452, and *m*/*z* 479, respectively. The peptidomimetic products were further modified to form desulfurized analogues in 16 additional steps as illustrated in Figure 4. MS spectra (Figure 5) of desulfurized A_1–B_1 (*m*/*z* 393), A_1–B_2 (*m*/*z* 419), A_2–B_1 (*m*/*z* 421), and A_2–B_2 (*m*/*z* 447) demonstrated that the starting materials were fully consumed. NMR spectra of desulfurized products formed by digital microfluidics were nearly identical to those formed using bench-scale techniques (Figure 6), with peaks at 4.05 and 4.29 ppm, characteristic of the reduced amide bond. A peak at 1.44 ppm and a group of peaks from 7.60–7.17 ppm confirmed both ligation ends (i.e., the Boc-protecting group and the phenyl group, respectively).

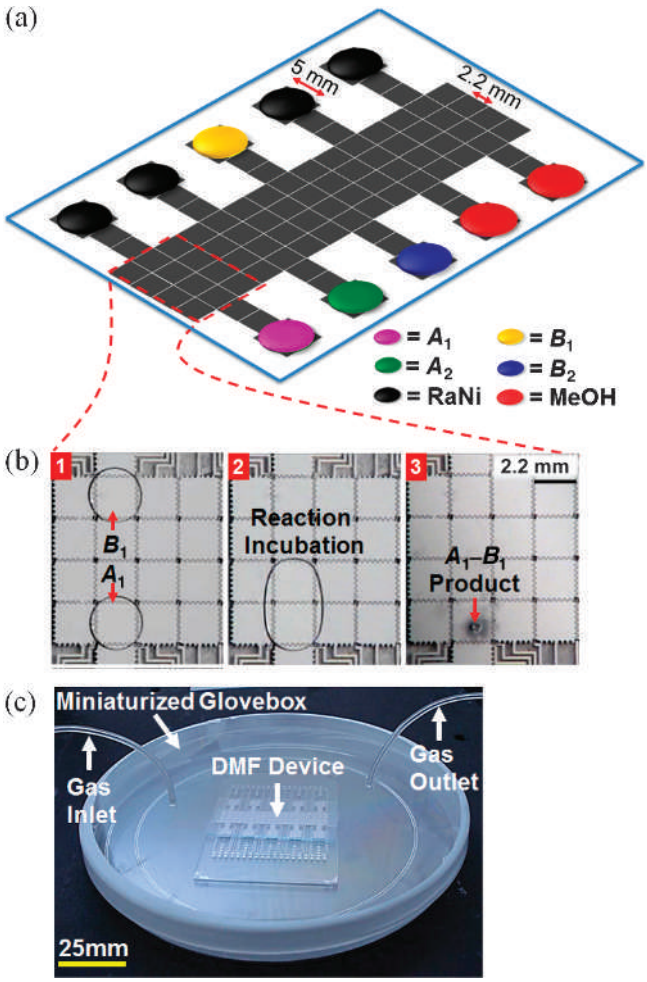

Figure 2. (a) Schematic of the digital microfluidic device used for combinatorial peptidomimetic ligation. (b) Sequence of frames from a movie illustrating digital microfluidic-based ligation. In frames 1 and 2, droplets containing thioacid peptides A_1 and NH aziridine-terminated amino acid B_1 were dispensed from their respective reservoirs, merged, mixed, and reacted in a miniaturized glovebox. Finally, in frame 3, peptidomimetic product A_1–B_1 was isolated by allowing the solvent to evaporate. (c) Picture of a miniaturized Petri-dish glovebox accommodating reactions under N_2

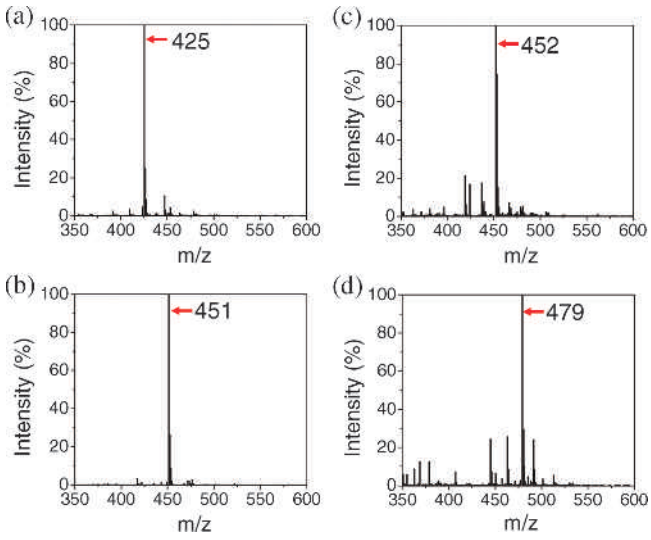

Figure 3. ESI-MS spectra of peptidomimetic products (a) A_1–B_1, (b) A_1–B_2, (c) A_2-B_1 and (d) A_2-B_2 synthesized by digital microfluidics

The new digital microfluidic method has several advantages relative to conventional techniques. This method delivers faster reactions and represents a >1000-fold reduction in reagent use relative to lab-scale methods (microliters relative to milliliters). In addition, the digital microfluidic method has the advantage of simplicity—no stir bars, stir plates, rotary evaporators, or (traditional) gloveboxes were required. The small footprint of the devices made it straightforward to fashion a miniaturized glovebox (Figure 2c) for implementing reactions under an inert atmosphere.

A critical step for many synthetic protocols (including those described here) is the removal of solvent, collection of some of

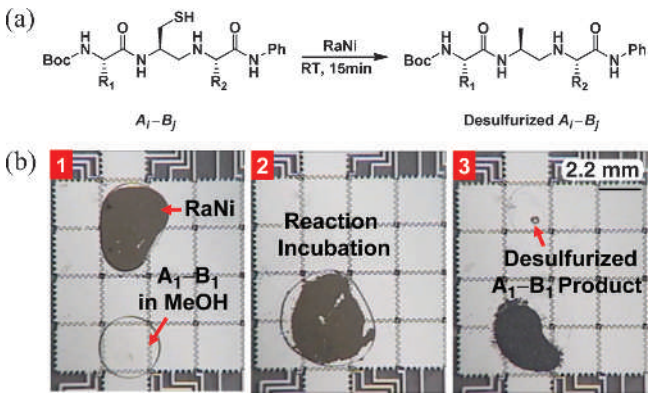

Figure 4. (a) Catalysis of desulfurization with Raney Nickel (RaNi). (b) Sequence of frames from a movie illustrating the steps of desulfurization with RaNi on a digital microfluidic device. In frames 1 and 2, peptidomimetic products are solubilized in methanol, merged with droplets of RaNi, and then incubated for 15 min at room temperature. In frame 3, desulfurized products were isolated by immobilizing the Ni with a magnet (not shown) and driving the reaction mixture away to evaporate

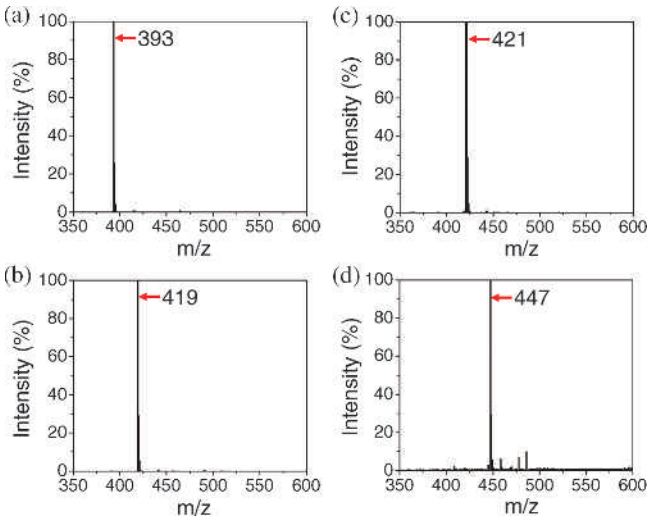

Figure 5. ESI-MS spectra of desulfurized peptidomimetic compounds (a) A_1–B_1, (b) A_1–B_2, (c) A_2–B_1 and (d) A_2–B_2 synthesized by digital microfluidics

the intermediate products for analysis, and re-dissolution for further processing. These steps can be challenging to implement in enclosed microchannels, but digital microfluidics is well-suited for forming precipitates and dissolving them [13c, 15]. Moreover, the reconfigurability of digital microfluidics allows for flexible solvent metering. In preliminary work, we found that 900-nL droplets of solvent were adequate to dissolve each of the peptidomimetic solids formed here, but in future experiments, much larger volumes (up to hundreds of microliters [16]) could be used depending on the solubility of each compound.

A significant novelty in the methods described here is the use of magnetic forces to separate a RaNi catalyst (composed of grains of nickel-aluminium alloy) from desulfurized products. In this process, a magnet was used to immobilize RaNi to the device surface and supernatant containing products was driven away using digital microfluidics (Figure 4). Magnetically controlled catalysts are currently attracting attention in the chemical synthesis community [17] because of the ease of recovery and reuse of catalyst materials. As far as we are aware, the methods reported here represent the first combination of magnetic isolation of inorganic catalysts implemented by microfluidics (of any format). We propose that this represents an important step forward for the field, as there is great potential for the development of rapid, automated synthesis with reusable magnetic catalytic materials (e.g., MagTrieve™ catalysts).

Finally, despite great promise, we observe that the microfluidic literature contains only a few references [4] to combinatorial synthesis because of the challenges inherent in such systems for controlling many different reagents. This is the first paper to report a digital microfluidic combinatorial synthesis. In this method, combinatorial techniques were applied to form eight products (typified by the spectra in Figures 3 and 5) in a total of 32 processing steps. This proof-of-concept is likely just the beginning; by increasing device footprint and/or operating multiple devices in parallel, we propose that it will be straightforward to synthesize tens of products in parallel. Furthermore, we envision future methods coupled with solid-phase extraction [18], separations [19], mass spectrometry [20], or multiplexed cell-based assays for bioactivity [21] which would allow for in-line analysis and screening.

3. Conclusions

In summary, we report a new microfluidic technique for combinatorial synthesis, applied to formation of peptidomimetics and their desulfurized analogues. This method strengthens the prospects of peptidomimetics for discovery of novel protein scaffolds and therapeutics. The new method has several advantages over bench-scale formats, including reduced reagent and sample consumption, automated handling of liquids and solids, and straightforward parallel-scale synthesis. The results suggest that there is great potential for digital microfluidics for fast and automated combinatorial synthesis of libraries of compounds.

4. Experimental

4.1. Reagents and Materials. Unless indicated otherwise, all reagents were obtained from Sigma Chemical (Oakville, ON). Deuterated methanol (MetOH-d4) was obtained from Cambridge Isotope Laboratories (Andover, MA). The starting materials (thioacid peptides and NH aziridine-terminated amino acids) shown in Figure 1 were synthesized using methods reported previously [14]. In all experiments, organic solvents were HPLC-grade.

4.2. Device Fabrication and Operation. The digital microfluidic devices used here are identical to those described elsewhere [13c, 22]. Briefly, the devices included a bottom plate bearing patterned chromium electrodes and a top plate bearing a contiguous indium tin oxide (ITO) electrode. The bottom plate featured an array of eighty-eight square actuation electrodes (2.2×2.2 mm with 140 μm peak to peak sinusoid interdigitated borders) connected to ten reservoir electrodes (5×5 mm ea.),

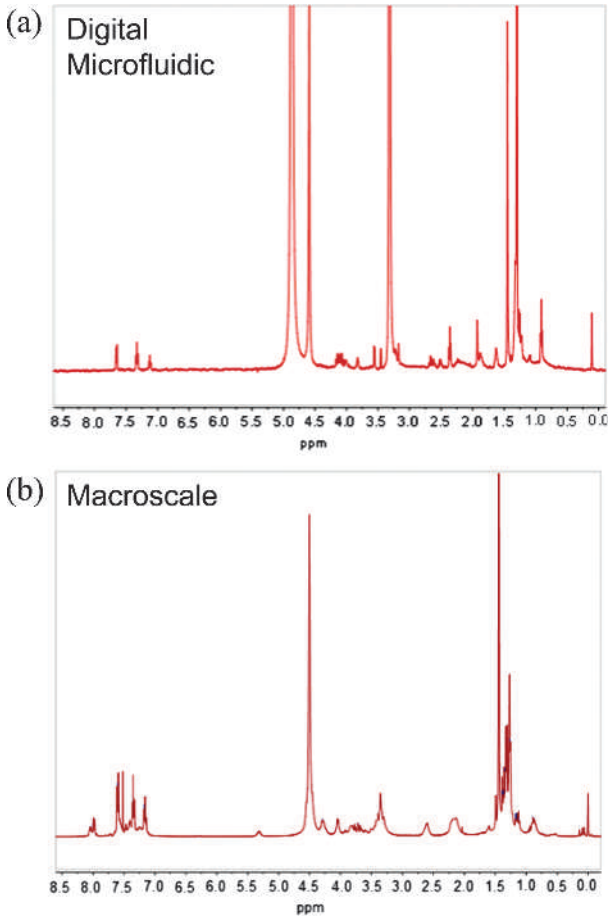

Figure 6. NMR spectra of desulfurized peptidomimetic compound A_1–B_1 synthesized by (a) digital microfluidics and (b) macroscale techniques. ^{1}H NMR (CD3OD, 400 MHz) δ: 8.04 (m, 0.12 H), 7.99 (d, J=7.7, 0.16 H), 7.60, (m, 2 H),7.35 (m, 2 H), 7.17 (m, 1 H), 4.29 (m, 1 H), 4.05 (d, J=6.8, 1 H), 3.83 (m, 1 H), 3.68 (m, 1 H), 3.50 (m, 1 H), 2.60 (m, 1 H), 2.16 (m, 3 H), 1.44 (m, 9 H), 1.31 (m, 6 H), 1.16 (m, 1 H), 0.89 (m, 1 H)

with inter-electrode gaps of 40 μm. Devices were assembled with the top plate and bottom plate separated by a spacer formed from two pieces of double-sided tape (total spacer thickness 180 μm). Each top plate was oriented such that the top-plate edges roughly aligned with the outer-edges of the reservoir electrodes on the bottom plate. Unit droplet and reservoir droplet volumes on these devices were ~900 nL and ~4.5 μL, respectively.

Driving potentials (70–100 VRMS) were generated by amplifying the sine-wave output of a function generator (Agilent Technologies, Santa Clara, CA) operating at 18 kHz. Reagents were loaded into reservoirs by pipetting an aliquot onto the bottom plate at the edge of the top plate and simultaneously applying driving potential to the closest reservoir electrode (relative to the top plate electrode) to draw the fluid into the reservoir. Thereafter, droplets were dispensed and actuated by applying driving potentials between the top electrode and sequential electrodes on the bottom plate. Droplet actuation was monitored and recorded by a CCD camera mounted with a lens.

A miniaturized glovebox was constructed from a polystyrene Petri dish (150 o.d. x 15 mm h). Two holes (~4 mm diameter ea.) were drilled through the lid and fitted with 10-cm long tubes (3 mm o.d.) and sealed using UV-curable LePage epoxy adhesive (Henkel Canada, Oakville, ON). In typical experiments, after droplet manipulation was completed, a digital microfluidic device was positioned in the modified Petri dish, which was then sealed with parafilm. The chamber was purged with N2 (~50 mL/min for 2 min). After purging, the inlet and outlet tube openings were closed and sealed with parafilm.

4.3. Digital Microfluidic Synthesis. Combinatorial peptidomimetic ligation was implemented in 16 steps (4 steps each to produce the 4 products shown in Figure 2 in the main text). First, eight 900-nL droplets containing the starting materials (two droplets each of A1, A2, B1, and B2, all 0.1 M in MeOH) were dispensed from their respective reservoirs. Second, a droplet of each starting reagent was merged with each corresponding reagent (i.e., A1 with B1, A1 with B2, A2 with B1, and A2 with B2). Third, the merged droplets were mixed (60 s, RT) by actuating in a circular motion on four electrodes and incubated (1 h) in a miniaturized glovebox under N2. Fourth, after the reaction, the device was removed from the glovebox and the top plate was removed to allow the solvent to evaporate (15 min, RT).

Some products were re-dissolved in an appropriate solvent and collected by pipette for off-chip analyses, while others were subsequently desulfurized on-chip in a second 16-step process (4 steps each to produce 4 desulfurized peptidomimetics). First, the top plate was replaced, and peptidomimetic products were resolubilized by dispensing 900-nL droplets of MeOH and driving them to the dried spots. Second, four reservoir-volume droplets (4.5 μL) containing Raney Nickel (~5 mg in MeOH) were dispensed and merged with each peptidomimetic product droplet. Third, the combined droplets were mixed (60 s, RT), incubated (15 min, RT), and the desulfurized products were isolated using a Neodymium Iron Boron magnet (Main Electronics, BC) to immobilize the nickel to the device surface. Fourth, the supernatant was driven away, the top plate was removed, and the solvent was allowed to evaporate (30 min, RT). The device top plate was removed, products were dissolved in appropriate solvent and collected by pipette for analysis. Macroscale synthesis of the same compounds was implemented as described previously [3].

4.4. Characterization. For analysis by mass spectrometry, ~2.3-mM solutions of reaction products formed by digital microfluidics were dissolved in 70-μL aliquots of methanol containing 0.1 % formic acid. These solutions were injected into a 1200 series quadrupole mass spectrometer (Agilent, Santa Clara, CA) operating in positive ion mode. The samples were delivered at a flow rate of 0.5 mL/min, with an applied voltage of 50 V and capillary temperature of 100 °C. Spectra were collected as an average of 67 acquisitions, and the data shown (Figures 3 and 5) are representative of analysis of products formed in triplicate.

For analysis by nuclear magnetic resonance (NMR), ~1.2-mM solutions of desulfurized peptidomimetic products generated by digital microfluidics were suspended in 80-μL aliquots of MeOH-d4 and transferred into a capillary tube (100 μm i.d.). The tube was sealed using a hand-held butane torch and positioned in a 3-mm Norell S400 NMR tube. 1 H-NMR spectra were collected using a Varian UnityPlus 500 MHz NMR spectrometer referenced to MeOH-d4 (3.31 ppm). 1 H-NMR spectra were recorded at 25 °C with a 16 ppm with 1-second recycle delay and 1 steady state, and 512 scans using 90-degree pulse width (7.3 μs). For analysis of reaction products synthesized by macroscale, samples were prepared in 3-mm tubes, and 1 H spectra were recorded on a Varian Mercury 400 MHz spectrometer. Spectra representative of products formed in triplicate are shown in Figure 6.

Acknowledgement. We thank the Natural Science and Engineering Research Council (NSERC) and Canadian Institutes of Health Research (CIHR) for financial support. We thank Timothy Burrow and Dmitry Pichugin for assistance with NMR analysis. A.R.W. thanks the Canada Research Chair (CRC) program for a CRC.

References

1. Gentilucci, L.; de Marco, R.; Cerisoli, L. *Curr. Pharm. Des*, **2010**, *16*, 3185–3203.
2. Vagner, J.; Qu, H.; Hruby, V. J. *Curr. Opin. Chem. Biol*. **2008**, *12*, 292–296.
3. (a) Assem, N.; Natarajan, A.; Yudin, A. K. *Am. Chem. Soc*. **2010**, *132*, 10986–10987; (b) Assem, N.; Yudin, A. K. *Nat. Proc*. **2012**, *7*, 1327–1334.
4. (a) Kikutani, Y.; Horiuchi, T.; Uchiyama, K.; Hisamoto, H.; Tokeshi, M.; Kitamori, T. *Lab Chip* **2002**, *2*, 188–192; (b) Wang, Y. J.; Lin, W. Y.; Liu, K.; Lin, R. J.; Selke, M.; Kolb, H. C.; Zhang, N. G.; Zhao, X. Z.; Phelps, M. E.; Shen, C. K. F.; Faull, K. F.; Tseng, H. R. *Lab Chip* **2009**, *9*, 2281–2285.
5. (a) Jahnisch, K.; Hessel, V.; Lowe, H.; Baerns, M. *Angew. Chem.-Int. Edit*. **2004**, *43*, 406–446; (b) Gunther, A.; Jensen, K. F. *Lab Chip* **2006**, *6*, 1487–1503; (c) Mason, B. P.; Price, K. E.; Steinbacher, J. L.; Bogdan, A. R.; McQuade, D. T. *Chem. Rev.* **2007**, *107*, 2300–2318; (d) DeMello, A. J. *Nature* **2006**, *442*, 394–402.
6. (a) Fernandez-Suarez, M.; Wong, S. Y. F.; Warrington, B. H. *Lab Chip* **2002**, *2*, 170–174; (b) Garcia-Egido, E.; Spikmans, V.; Wong, S. Y. F.; Warrington, B. H. *Lab Chip* **2003**, *3*, 73–76.
7. He, J.; Du, Y.; Guo, Y.; Hancock, M. J.; Wang, B.; Shin, H.; Wu, J.; Li, D.; Khademhosseini, A. *Biotechnol. Bioeng*. **2011**, *108*, 175–185.
8. Toyota, A.; Nakamura, H.; Ozono, H.; Yamashita, K.; Uehara, M.; Maeda, H. *J. Phys. Chem. C*. **2010**, *114*, 7527–7534.
9. (a) Sista, R. S.; Eckhardt, A. E.; Wang, T.; Graham, C.; Rouse, J. L.; Norton, S. M.; Srinivasan, V.; Pollack, M. G.; Tolun, A. A.; Bali, D.; Millington, D. S.; Pamula, V. K. *Clin. Chem.* **2011**, *57*, 1444–1451; (b) Perry, G.; Thomy, V.; Das, M. R.; Coffinier, Y.; Boukherroub, R. *Lab Chip* **2012**, *12*, 1601–1604; (c) Wijethunga, P. A. L.; Nanayakkara, Y. S.; Kunchala, P.; Armstrong, D. W.; Moon, H. *Anal. Chem.* **2011**, *83*, 1658–1664; (d) Yang, H.; Mudrik, J. M.; Jebrail, M. J.; Wheeler, A. R. *Anal. Chem*. **2011**, *83*, 3824–3830.
10. (a) Lee, J. N.; Park, C.; Whitesides, G. M. *Anal. Chem*. **2003**, *75*, 6544–6554; (b) Whitesides, G. M. *Nature* **2006**, *442*, 368–373.
11. Wang, J. Y.; Sui, G. D.; Mocharla, V. P.; Lin, R. J.; Phelps, M. E.; Kolb, H. C.; Tseng, H. R. *Angew. Chem.-Int. Edit.* **2006**, *45*, 5276–5281.
12. (a) Jebrail, M. J.; Bartsch, M. S.; Patel, K. D. *Lab Chip* **2012**, *12*, 2452–2463; (b) Jebrail, M. J.; Wheeler, A. R. *Curr. Opin. Chem. Biol*. **2010**, *14*, 574–581; (c) Wheeler, A. R. *Science* **2008**, *322*, 539–540.
13. (a) Millman, J. R.; Bhatt, K. H.; Prevo, B. G.; Velev, O. D. *Nat. Mater.* **2005**, *4*, 98–102; (b) Dubois, P.; Marchand, G.; Fouillet, Y.; Berthier, J.; Douki, T.; Hassine, F.; Gmouh, S.; Vaultier, M. *Anal. Chem*. **2006**, *78*, 4909–4917; (c) Jebrail, M. J.; Ng, A. H. C.; Rai, V.; Hili, R.; Yudin, A. K.; Wheeler, A. R. *Angew. Chem.-Int. Edit*. **2010**, *49*, 8625–8629; (d) Baker, C. A.; Roper, M. G. *Anal. Chem*. **2012**, *84*, 2955–2960; (e) Witters, D.; Vergauwe, N.; Ameloot, R.; Vermeir, S.; De Vos, D.; Puers, R.; Sels, B.; Lammertyn, J. *Adv. Mater.* **2012**, *24*, 1316–1320; (f) Keng, P. Y.; Chen, S.; Ding, H.; Sadeghi, S.; Shah, G. J.; Dooraghi, A.; Phelps, M. E.; Satyamurthy, N.; Chatziioannou, A. F.; Kim, C. J.; Van Dam, R. M. *Proc. Natl. Acad. Sci.* **2012**, *109*, 690–695.

14. (a) Hili, R.; Yudin, A. K. *J. Am. Chem. Soc.* **2006**, *128*, 14772–14773; (b) Li, X.; Yudin, A. K. *J. Am. Chem. Soc.* **2007**, *129*, 14152–14153.
15. Jebrail, M. J.; Wheeler, A. R. *Anal. Chem.* **2009**, *81*, 330–335.
16. Au, S. H.; Shih, S. C. C.; Wheeler, A. R. *Biomed. Microdevices* **2011**, *13*, 41–50.
17. Polshettiwar, V.; Luque, R.; Fihri, A.; Zhu, H.; Bouhrara, M.; Basset, J. M. *Chem. Rev.* **2011**, *111*, 3036–3075.
18. Yang, H.; Mudrik J. M.; Jebrail M. J.; Wheeler, A. R. *Anal. Chem.* **2011**, *83*, 3824–3830.
19. Watson, M. W. L.; Jebrail, M. J.; Wheeler, A. R. *Anal. Chem.* **2010**, *82*, 6680–6686.
20. (a) Jebrail, M. J.; Yang, H.; Mudrik, J. M.; Lafreniere, N. M.; McRoberts, C.; Al-Dirbashi, O. Y.; Fisher, L.; Chakraborty, P.; Wheeler, A. R. *Lab Chip* **2011**, *11*, 3218–3224; (b) Shih, S. C. C.; Yang, H.; Jebrail, M. J.; Fobel, R.; McIntosh, N.; Al-Dirbashi, O. Y.; Chakraborty, P.; Wheeler, A. R. *Anal. Chem.* **2012**, *84*, 3731–3738.
21. Bogojevic, D.; Chamberlain, M. D.; Barbulovic-Nad, I.; Wheeler, A. R. *Lab Chip* **2012**, *12*, 627–634.
22. Jebrail, M. J.; Luk, V. N.; Shih, S. C. C.; Fobel, R.; Ng, A. H. C.; Yang, H.; Freire, S. L. S.; Wheeler, A. R. *J. Vis. Exp.* **2009**, e1603, DOI: 1610.3791/1603.